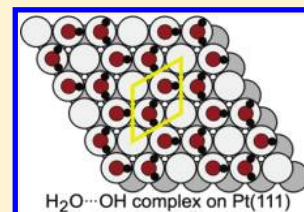


The Energy of Hydroxyl Coadsorbed with Water on Pt(111)

Wanda Lew,[†] Matthew C. Crowe,[†] Charles T. Campbell,^{*,†} Javier Carrasco,^{‡,§,||} and Angelos Michaelides[‡][†]Department of Chemistry, University of Washington, Seattle, Washington 98195-1700, United States[‡]London Centre for Nanotechnology and Department of Chemistry, University College London, London WC1E 6BT, U.K.[§]Fritz-Haber-Institut der Max-Planck-Gesellschaft, Faradayweg 4-6, 14195 Berlin, Germany^{||}Instituto de Catálisis y Petroleoquímica, CSIC, Marie Curie 2, E-28049 Madrid, Spain**S** Supporting Information

ABSTRACT: Adsorbed OH is a key intermediate in many catalytic reactions and a common species on many materials' surfaces. We report here measurements of the calorimetric heats for forming the widely studied and structurally well-defined coadsorbed (H₂O···OH) complex on Pt(111) from water vapor and adsorbed oxygen adatoms. We further use these heats as benchmarks to evaluate the performance of density functional theory, modified to include van der Waals interactions and zero-point energies, and find agreement to within 1 and 15 kJ/mol for the two adlayer structures studied.



INTRODUCTION

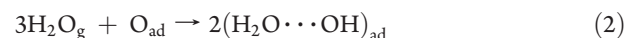
Adsorbed hydroxyl (OH_{ad}) is a key intermediate in many catalytic reactions over transition metals. For Pt, these include oxidations of organic molecules, steam reforming of hydrocarbons and oxygenates, decomposition of oxygenates, and water gas shift. As a result, and because of the very common presence of OH_{ad} on the surfaces of many materials, a considerable body of work has gone into understanding the properties of OH_{ad}.¹ However, despite its great importance, an absolutely key quantity, namely, the energy of adsorbed hydroxyl, has not yet been measured on any surface except for our earlier heat measurements of one of the two surface structures discussed here.² One of the most widely studied and well-defined structures of OH_{ad} on any surface is the coadsorbed OH–H₂O overlayer that forms on Pt(111).¹ This overlayer, produced by coadsorbing H₂O and oxygen^{1,3–8} or through reaction of H₂ plus O₂,^{6,7,9} therefore, presents an excellent opportunity to establish the stability of OH_{ad} on a transition-metal surface.

When water gas is dosed to preadsorbed O adatoms on Pt(111), adsorbed hydroxyl groups are produced.^{1,3–8} In principle, the simplest reaction to give OH_{ad} would be with a 1:1 stoichiometry



where the subscripts *g* and *ad* indicate gas-phase and adsorbed species, respectively. However, it is now established that the reaction of H₂O_g and O_{ad} is not this simple and, instead, a coadsorbed, hydrogen-bonded H₂O···OH complex with a $\sqrt{3}$ or 3×3 crystalline overlayer is formed.^{1,3,4} It is most stable against decomposition to H₂O_g plus O_{ad} when formed with a ratio of 3H₂O:1O_{ad}, where it remains stable upon heating in ultrahigh vacuum up to 205 K.^{1,3,4} This 3H₂O:1O_{ad} ratio indicates that the most stable complex has a 1:1 ratio of H₂O/OH, implying a complex of the form (H₂O···OH)_{ad}. Clay et al.³

found that the amount of reacted water at 163 K versus the amount of preadsorbed O is best described by the following reaction stoichiometry:



Both low-energy electron diffraction (LEED) and scanning tunneling microscopy (STM) measurements show that the H₂O + O_{ad} reaction produces islands of either a $\sqrt{3}$ or a 3×3 structure, or both, depending on the conditions of production, in either case with a local coverage of 2/3 ML of O atoms total.^{1,3–5} For the $\sqrt{3}$ structure, this can only be rationalized with one H₂O_{ad} and one OH_{ad} per unit cell, consistent with the (H₂O···OH)_{ad} complex of reaction 2. The structures of these $\sqrt{3}$ and 3×3 overlayers, as computed with DFT,^{10–13} are consistent with this composition as well as LEED and STM results¹ (Figure 1). The structures consist of hexagonal hydrogen-bonded networks of H₂O and OH bonded to the Pt atop sites and differ only in their H-bond topologies.

Here, we report calorimetric measurements of the heat of forming this well-defined (H₂O···OH)_{ad} complex on Pt(111) from water plus adsorbed O in two different adlayer structures and compare these measured energies to new DFT calculations of these structures. These are the first experimental determinations of the energies of any well-defined adsorbed hydroxyl structure on any surface, except for our earlier paper describing heat measurements of one of the two adlayer structures presented here.² In that earlier paper, we did not discuss the details of the structures nor the DFT energies of either adlayer whose structures and energies we analyze here. This is also one of the only calorimetric measurements of the energy of any well-defined adlayer structure where the adlayer is stabilized by hydrogen

Received: August 1, 2011**Revised:** October 1, 2011**Published:** October 04, 2011

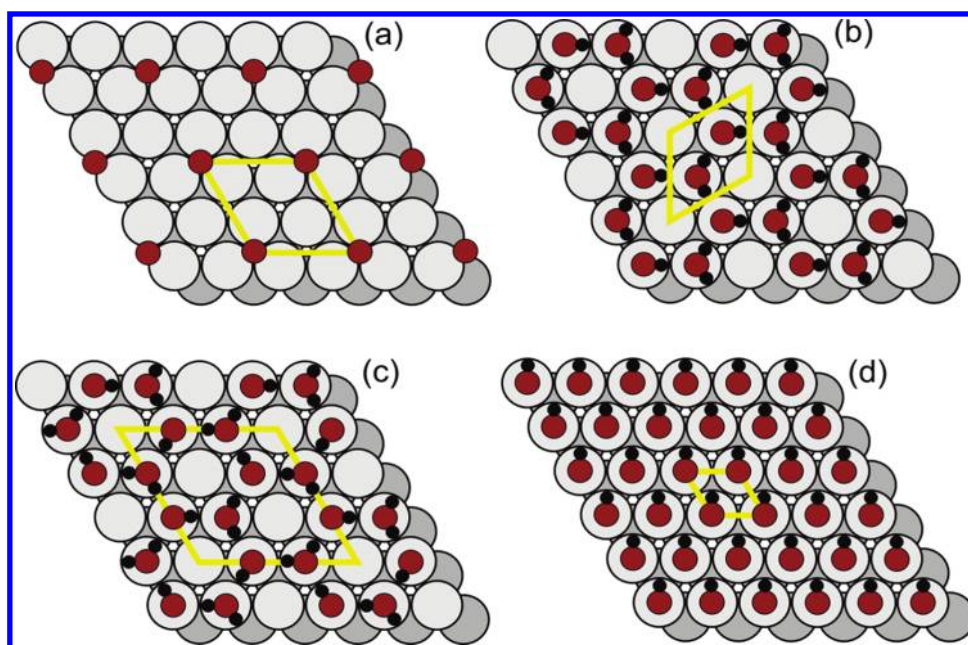


Figure 1. Top view of adsorbate-covered Pt(111) models: (a) $\text{O}_{\text{ad},2\times 2}$, (b) $(\text{H}_2\text{O}\cdots\text{OH})_{\text{ad},\sqrt{3}\times\sqrt{3}}$, (c) $(3\text{H}_2\text{O}\cdots 3\text{OH})_{\text{ad},3\times 3}$, and (d) $\text{OH}_{\text{ad},1\times 1}$. The unit cell is in yellow. Open and gray-filled circles represent Pt atoms. Red and smaller black circles represent O and H atoms, respectively.

bonding.¹⁴ Not only are these valuable energy measurements in their own right but also they provide important benchmarks against which to evaluate the accuracy of DFT, a very active research focus in surface and materials science. Here, we use these measured energies as such a benchmark, comparing them to results with both a standard semilocal functional and a non-local functional that accounts for van der Waals dispersion forces.^{15,16} We find that, when these forces are included, the agreement is within 15 and 1 kJ/mol for the structures studied, quite good given the large errors sometimes seen with standard DFT.¹⁷

EXPERIMENTAL SECTION

Experiments were performed in an ultra-high-vacuum chamber (base pressure $< 2 \times 10^{-10}$ mbar) with capabilities for single-crystal adsorption microcalorimetry and surface analysis described previously.¹⁸ Methods were the same as those reported there. The error in absolute accuracy of the calorimetric heats (when averaging >3 independent runs as here) is estimated to be $<3\%$ for systems like those here with sticking probabilities above 0.8.¹⁹ We estimate that the additional error associated with the scatter in O adatom precoverages increases this heat error to $\sim 5\%$. More details of sample surface preparation, sticking probability measurements, and heat measurements are presented elsewhere, where results are also presented for a wider range of O and water coverages.^{2,19} Experiments were performed with D_2O rather than H_2O to improve accuracy in measuring large sticking probabilities by mass spectrometry. O adatoms were produced by dosing O_2 gas to Pt(111) at 150 K.

COMPUTATIONAL METHODS

DFT calculations were performed with the VASP 5.2 code.^{20,21} Two exchange-correlation functionals were used: the semilocal PBE²² and an offspring of the nonlocal van der Waals density functional (vdW-DF) of Dion et al.,¹⁵ referred to as “optB88-vdW”.¹⁶ The difference between the original vdW-DF of Dion et al. and

Table 1. Calorimetrically Measured Reaction Enthalpies (Integral Heats of D_2O Adsorption) at 150 K for the Stated Reactant Coverages

	reacted amounts	reaction enthalpy (kJ/mol D_2O)
reaction 2	1/6 ML O_{ad} + 1/2 ML D_2O	-57.4 ± 2.9
reaction 3	1/4 ML O_{ad} + 1/2 ML D_2O	-60.2 ± 3.0

optB88-vdW is merely in the exchange functional, with the optB88 exchange functional yielding more accurate interaction energies than the original choice of revPBE.¹⁶ Indeed, the optB88-vdW and the other optimized vdW density functionals reported in ref 16 have now been successfully applied to a wide variety of systems, for example, to bulk solids,^{23,24} hydrocarbon and noble gas adsorption on metals,^{25,26} and water adsorption and water clusters.^{16,27,28}

The computational setup is similar to our previous works.^{27,28} Valence electronic states were expanded in plane waves with a cutoff energy of 500 eV, and a Monkhorst–Pack grid with $12 \times 12 \times 1$ k -point sampling per (1×1) unit cell was used. The Pt(111) surface was modeled by $(\sqrt{3} \times \sqrt{3})$ and (3×3) unit cells, containing six atomic layers. The atoms in the three bottom layers were fixed to their bulk-truncated PBE positions ($a_{\text{Pt}} = 3.981$ Å) during structure optimizations. In all cases, a dipole correction along the direction perpendicular to the metal surface was applied and geometry optimizations were performed with a residual force threshold of 0.015 eV/Å. Zero-point energies were obtained by computing the vibrational frequencies of the adsorbed species by means of a finite displacement method.

RESULTS

We measured the energy of reaction 2 using calorimetry at 150 K²⁹ and two O_{ad} precoverages (1/6 and 1/4 ML) chosen to give the best comparisons to previous experiments that gave well-defined LEED and STM structures. Table 1 presents the integral heats of adsorption for D_2O at these precoverages for 1/2 ML of reacted D_2O . The first entry is for $\sim 1/6$ ML of O_{ad} ,³⁰ which gives

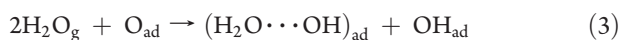
Table 2. Reaction Energies per Mole of Reacted H₂O and D₂O (ΔE) Corresponding to Reactions 2C–4C Computed with PBE and optB88-vdW^a

reaction	ΔE (kJ/mol of H ₂ O)		ΔE^{ZPE} (kJ/mol of H ₂ O)		ΔE^{ZPE} (kJ/mol of D ₂ O)		ΔH^{ZPE} at 150 K (kJ/mol of D ₂ O)
	PBE	optB88-vdW	PBE	optB88-vdW	PBE	optB88-vdW	optB88-vdW
2C	−59.1 (−60.2)	−81.6 (−82.7)	−49.8 (−51.2)	−71.9	−51.7	−73.8	−75.0
3C	−40.5 (−41.3)	−65.5 (−66.3)	−32.0 (−33.0)	−56.7	−33.7	−58.5	−59.7
4C	+15.3	−17.0	+21.6	−11.2	+20.4	−12.3	−13.5

^a Zero-point energy corrected energies are also shown (ΔE^{ZPE}). For reactions 2C and 3C, a $\sqrt{3}$ model was used for the H₂O–OH overlayer. Values in parentheses were computed using its 3×3 model.

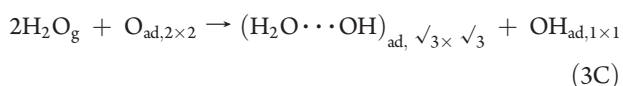
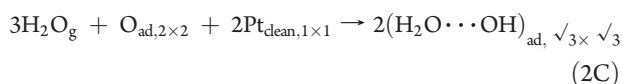
the 1:1 (D₂O···OD)_{ad} complex with 2/3 ML of O atoms total local coverage, completely covering the Pt with no other coadsorbates. This is the best condition to study reaction 2 cleanly and get the most product. For these conditions, the complex is expected to be in its $\sqrt{3}$ structure.^{3,4} (Note that this D₂O coverage is about 20% below saturation,² and the 3×3 appears only closer to saturation.^{3,4}) The measured enthalpy change for this reaction is −57.4 kJ per mol of reacted D₂O, or −172.2 kJ per mol, as written in reaction 2.

The second entry in Table 1 is for the most commonly reported experimental condition for producing the (H₂O···OH)_{ad} complex, which involves reacting 1/2 ML of water vapor with 1/4 ML O_{ad} in its p(2 × 2) structure.^{1,3–8,31–35} The net reaction under these conditions is



This reaction is more complicated since there is too much O to cover the whole surface in the (H₂O···OH)_{ad} complex, so additional OH_{ad} is also produced. Under these conditions, STM studies⁷ show that, in addition to large regions of the $\sqrt{3}$ structure (later proven to be (H₂O···OH)_{ad}), this reaction leads to smaller domains (chains between the domains) attributed to a pure OH_{ad} phase with 1 ML local OH coverage. Thus, this condition produces 1/4 ML of the (H₂O···OH)_{ad} together with 1/4 ML of coadsorbed OH_{ad} in domains of pure OH at 1 ML local coverage (which we, therefore, model here as p(1 × 1) domains, neglecting interactions at the edges of these chainlike domains), as in reaction 3 above. This p(1 × 1)-OH structure is consistent with the stoichiometry of the excess reactants (beyond those used to make the (H₂O···OH)_{ad} complex) at this lower water/O_{ad} reactant ratio. Still, it is supported by less evidence than the $\sqrt{3}$ structure. The total O atom coverage is 3/4 ML in these combined $\sqrt{3}$ -(D₂O···OD) plus p(1 × 1)-OD structures, with the latter domains covering one-fourth of the surface and the $\sqrt{3}$ -(D₂O···OD) domains covering the remaining three-quarters of the surface with a local coverage of 1/3 ML of (D₂O···OD)_{ad}. The measured enthalpy change for this reaction is −60.2 kJ per mol of reacted D₂O.

With DFT, we computed the energy change of H₂O_g reacting with O_{ad} on Pt(111) to produce several H₂O/OH overlayers, with different water and O adatom stoichiometries. On the basis of the established structure of the $\sqrt{3}$ -(H₂O···OH) overlayer, the precise reactions and structural models that best mimic the experiments are



The reaction numbers here correspond to the same basic reactions as above, but the “C” implies a computed reaction, which requires more strict limitation to these specific initial and final structures. These structural models are shown schematically in Figure 1. (Exact atomic coordinates are given in the Supporting Information; see below.) In these reactions, “O_{ad,2 × 2}” represents regions of O-covered Pt in the (2 × 2) structure (Figure 1a) and “Pt_{clean,1 × 1}” represents adsorbate-free Pt sites. Details of reaction energies are given in ref 36.

Reaction 3C involves an initial H₂O-to-O_{ad} stoichiometry of 2:1 and produces a mixture of the (H₂O···OH)_{ad} complex and pure OH_{ad} domains on the surface^{5,11} with an overall H₂O/OH ratio in the final adlayer of 1:2.³⁷ This reaction mimics as closely as possible the observed overlayer structure and stoichiometry of the experiments in ref 6. Reaction 2C involves an initial H₂O/O_{ad} stoichiometry of 3:1 and produces exclusively the mixed (H₂O···OH)_{ad} overlayer with exactly a 1:1 ratio. Notice that reaction 2C implies that only two-thirds of the total surface area is covered initially by (2 × 2)-O domains.

Reaction 2C mimics the higher initial H₂O/O_{ad} stoichiometry required to make a pure adlayer of the 1:1 (H₂O···OH)_{ad} complex in the $\sqrt{3}$ structure. Reaction 4C corresponds to the reaction of 1/4 ML of water with a p(2 × 2) layer of O_{ad} (1/4 ML) to form domains of the pure OH p(1 × 1) overlayer at 1 ML local coverage (Figure 1d) (in domains covering just half the surface, with the other half free of adsorbates):



We include it to show the relative stability of this pure OH overlayer within DFT, but it has not been observed experimentally on Pt(111) without also producing (H₂O···OH)_{ad}.

The calculated energies for these reactions are summarized in Table 2. It can be seen that the PBE and optB88-vdW results differ considerably, with the vdW functional yielding more favorable reaction energies (by 20–25 kJ/mol for reactions 2C and 3C). This is consistent with our recent work for water on metals, which has shown that vdW forces contribute substantially to the water–metal bond.²⁸ Zero-point energies obtained by the harmonic approximation also reduce reaction 2C's and 3C's energies by about 10 kJ/mol, but show only weak sensitivity to D vs H (<2 kJ/mol). Reactions 2C and 3C involve a $\sqrt{3}$ model of the (H₂O···OH) overlayer (Figure 1b). The reaction energies for the equivalent reactions, but going to the 3×3 structure (Figure 1c), yield very similar energies (within 1.5 kJ/mol), as shown in Table 2, with the 3×3 structure being slightly more stable than the $\sqrt{3}$ structure.

To compare the computed reaction energies at 0 K in Table 2 to the measured reaction enthalpies (ΔH) at 150 K in Table 1, one must subtract RT (1.2 kJ/mol at 150 K), neglecting differences in heat capacities. Table 2 also shows these estimates

of reaction enthalpies for the most accurate DFT method employed here, that is, the optB88-*vdW* functional. The experimental enthalpy for reaction 2 (-57.4 kJ/mol D_2O) is 17.6 kJ/mol less exothermic than the computed enthalpy for reaction 2C (-75.0 kJ/mol D_2O). However, because O_{ad} is less stable in the (2×2) -O domains of $1/4$ ML coverage as used in reaction 2C than when it is spread out evenly across the surface at lower local coverage ($1/6$ ML O) as in the experiment of reaction 2, we must add 3 kJ/mol D_2O to reaction 2C. (This correction equals the difference in the integral heat of O adsorption at these two coverages, 9 kJ/mol O_{ad} ³⁸ divided by 3 since reaction 2 has three D_2O molecules per O_{ad} .) This reduces the DFT enthalpy to -72.0 kJ/mol D_2O at the experimental coverage, leaving a 14.6 kJ/mol difference from the experimental value.

The measured enthalpy of -60.2 kJ/mol D_2O for reaction 3 in Table 1 is very close to the DFT enthalpy for reaction 3C in the last column of Table 2 of -59.7 kJ/mol D_2O . The discrepancy is <1 kJ/mol D_2O , which is likely to be to some extent fortuitous as this is beyond the accuracy expected for any DFT functional.

To summarize, the computed enthalpies differ by less than 15 and 1 kJ/mol D_2O from experimental measurements for reactions 2 and 3, respectively. Reaction 2's enthalpy is predicted to be 12 kJ/mol D_2O more exothermic than reaction 3 by DFT, whereas their experimental enthalpies are indistinguishable within the error bars. The experimental error bars in Table 1 do allow reaction 2 to be more exothermic than reaction 3 by up to 3.1 kJ/mol D_2O , so there is no qualitative error here. If we average both reactions 2 and 3, the DFT enthalpy of -65.8 kJ/mol agrees with the experimental average (-58.8 kJ/mol) to within 7 kJ/mol. This is very good agreement, especially in comparison to difficult cases, such as benzene and naphthalene on Pt, where semilocal DFT calculations give errors of 80 and 140 kJ/mol, respectively, relative to our heat of adsorption measurements.¹⁷ (We have not yet tried the optB88-*vdW* method used here for benzene on Pt.) The small residual error here may be due to a remaining inaccuracy of optB88-*vdW*, domain boundary effects, or because some of the adsorbed layer may not reach its most stable structure within the measurement time (~ 100 ms).

Here, we have directly probed the energetics of this system by calorimetry. Although temperature-programmed desorption (TPD) has been applied to this system,³ it gives large error bars in its activation energy in this case¹² and, even if determined accurately, would not give the net reaction energy measured here, since it would include the excess activation energy for adsorption. This could be large since a $DO-D$ bond is broken.

CONCLUSIONS

The generally very good agreement between the current calculations and experiments strongly supports the structural details for the overlayers provided by DFT. This is the first comparison of the computed energy of the water-OH overlayer to its experimental formation energy, and thus it provides the most stringent test of this structure reported. Together with these newly measured energies, this provides a deeper understanding of the structure and stability of the mixed OH-water overlayer. The combined calorimetric/computational approach used here has the potential to elucidate hydrogen bond strengths in other hydrogen-bonded overlayers and, more generally, to aid in the development of improved electronic structure methods for the calculation of adsorption and reaction at surfaces.

ASSOCIATED CONTENT

S Supporting Information. Exact atomic coordinates for the structures in Figure 1 are given in the Supporting Information. This material is available free of charge via the Internet at <http://pubs.acs.org>.

AUTHOR INFORMATION

Corresponding Author

*E-mail: campbell@chem.washington.edu.

ACKNOWLEDGMENT

The authors acknowledge support by NSF Grant CHE-1010287. J.C. has been supported by the Royal Society through a Newton International Fellowship, Matthias Scheffler at the Fritz Haber Institute, and the Spanish Ministerio de Ciencia e Innovación through a Ramón y Cajal Fellowship. A.M. is supported by the ERC. We are also grateful to the Materials Chemistry Consortium for time on HECToR (EPSRC Grant EP/F067496).

REFERENCES

- (1) Hodgson, A.; Haq, S. *Surf. Sci. Rep.* **2009**, *64*, 381.
- (2) Lew, W.; Crowe, M. C.; Karp, E.; Lytken, O.; Farmer, J. A.; Árnadóttir, L.; Schoenbaum, C.; Campbell, C. T. *J. Phys. Chem. C* **2011**, *115*, 11586.
- (3) Clay, C.; Haq, S.; Hodgson, A. *Phys. Rev. Lett.* **2004**, *92*, 046102.
- (4) Held, G.; Clay, C.; Barrett, S. D.; Haq, S.; Hodgson, A. *J. Chem. Phys.* **2005**, *123*, 64711.
- (5) Bedurftig, K.; Volkening, S.; Wang, Y.; Wintterlin, J.; Jacobi, K.; Ertl, G. *J. Chem. Phys.* **1999**, *111*, 11147.
- (6) Sachs, C.; Hildebrand, M.; Volkening, S.; Wintterlin, J.; Ertl, G. *J. Chem. Phys.* **2002**, *116*, 5759.
- (7) Sachs, C.; Hildebrand, M.; Volkening, S.; Wintterlin, J.; Jacobi, K.; Ertl, G. *Science* **2001**, *293*, 1635.
- (8) Seitsonen, A. P.; Zhu, Y. J.; Bedurftig, K.; Over, H. *J. Am. Chem. Soc.* **2001**, *123*, 7347.
- (9) Volkening, S.; Bedurftig, K.; Jacobi, K.; Wintterlin, J.; Ertl, G. *Phys. Rev. Lett.* **1999**, *83*, 2672.
- (10) Michaelides, A.; Hu, P. *J. Chem. Phys.* **2001**, *114*, 513.
- (11) Michaelides, A.; Hu, P. *J. Am. Chem. Soc.* **2001**, *123*, 4235.
- (12) Karlberg, G. S.; Wahnstrom, G.; Clay, C.; Zimbitas, G.; Hodgson, A. *J. Chem. Phys.* **2006**, *124*, 204712.
- (13) Karlberg, G. S.; Olsson, F. E.; Persson, M.; Wahnstrom, G. *J. Chem. Phys.* **2003**, *119*, 4865.
- (14) To our knowledge, the only previous case is our recent report of the energy of the $(\sqrt{37} \times \sqrt{37})R25.3^\circ$ structure of molecularly adsorbed water on Pt(111).¹⁹
- (15) Dion, M.; Rydberg, H.; Schröder, E.; Langreth, D. C.; Lundqvist, B. I. *Phys. Rev. Lett.* **2004**, *92*, 246401.
- (16) Klimeš, J.; Bowler, D. R.; Michaelides, A. *J. Phys.: Condens. Matter* **2010**, *22*, 022201.
- (17) Gottfried, J. M.; Vestergaard, E. K.; Bera, P.; Campbell, C. T. *J. Phys. Chem. B* **2006**, *110*, 17539.
- (18) Lew, W.; Lytken, O.; Farmer, J. A.; Crowe, M. C.; Campbell, C. T. *Rev. Sci. Instrum.* **2010**, *81*, 024102.
- (19) Lew, W.; Crowe, M. C.; Karp, E.; Campbell, C. T. *J. Phys. Chem. C* **2011**, *115*, 9164.
- (20) Kresse, G.; Furthmüller, J. *Phys. Rev. B* **1996**, *54*, 11169.
- (21) Kresse, G.; Hafner, J. *Phys. Rev. B* **1993**, *47*, 558.
- (22) Perdew, J. P.; Burke, K.; Ernzerhof, M. *Phys. Rev. Lett.* **1996**, *77*, 3865.
- (23) Klimeš, J.; Bowler, D. R.; Michaelides, A. *Phys. Rev. B* **2011**, *83*, 195131.

(24) Santra, B.; Klimeš, J.; Alfè, D.; Tkatchenko, A.; Slater, B.; Michaelides, A.; Car, R.; Scheffler, M. *Phys. Rev. Lett.*, in press.

(25) Addato, M. A. F.; Rubert, A. A.; Benitez, G. A.; Fonticelli, M. H.; Carrasco, J.; Carro, P.; Salvarezza, R. C. *J. Phys. Chem. C* **2011**, *115*, 17788.

(26) Zhang, Y. N.; Hanke, F.; Bortolani, V.; Persson, M.; Wu, R. Q. *Phys. Rev. Lett.* **2011**, *106*, 236103.

(27) Forster, M.; Raval, R.; Hodgson, A.; Carrasco, J.; Michaelides, A. *Phys. Rev. Lett.* **2011**, *106*, 046103.

(28) Carrasco, J.; Santra, B.; Klimeš, J.; Michaelides, A. *Phys. Rev. Lett.* **2011**, *106*, 026101.

(29) We noted elsewhere¹⁹ that 150 K here corresponds to 160 K in the papers by Hodgson's group^{3,4} due to systematic errors in thermocouples.

(30) Actually, this entry reports the average of several experimental runs that had an average O_{ad} precoverage of 0.18, with all precoverages being within 0.03 ML of that average.

(31) Fisher, G. B.; Gland, J. L. *Surf. Sci.* **1980**, *94*, 446.

(32) Fisher, G. B.; Sexton, B. A. *Phys. Rev. Lett.* **1980**, *44*, 683.

(33) Creighton, J. R.; White, J. M. *Surf. Sci.* **1982**, *122*, L648.

(34) Creighton, J. R.; White, J. M. *Chem. Phys. Lett.* **1982**, *92*, 435.

(35) Schiros, T.; Naslund, L. A.; Andersson, K.; Gyllenpalm, J.; Karlberg, G. S.; Odelius, M.; Ogasawara, H.; Pettersson, L. G. M.; Nilsson, A. *J. Phys. Chem. C* **2007**, *111*, 15003.

(36) Reaction 2C's energy is $2E^{tot}[(H_2O \cdots OH)_{ad,(\sqrt{3} \times \sqrt{3})}] - 3E^{tot}[H_2O_g] - E^{tot}[O_{ad,(2 \times 2)}] - 2E^{tot}[Pt_{clean,(1 \times 1)}]$, where E^{tot} for each surface species is the total energy per unit cell of that slab, for example, the $(H_2O \cdots OH)_{ad,(\sqrt{3} \times \sqrt{3})}$ slab for the first term and the (1×1) clean Pt slab for the last term, and $E^{tot}[H_2O_g]$ is the total energy of H_2O gas. Reaction 3C's energy is $E^{tot}[(H_2O \cdots OH)_{ad,(\sqrt{3} \times \sqrt{3})}] + E^{tot}[OH_{ad,(1 \times 1)}] - 2E^{tot}[H_2O_g] - E^{tot}[O_{ad,(2 \times 2)}]$. Reaction 4C's energy is $2E^{tot}[OH_{ad,(1 \times 1)}] + 2E^{tot}[Pt_{clean,(1 \times 1)}] - E^{tot}[H_2O_g] - E^{tot}[O_{ad,(2 \times 2)}]$.

(37) All calculations represent cases where all domains are so large that there are no edge effects.

(38) Fiorin, V.; Borthwick, D.; King, D. A. *Surf. Sci.* **2009**, *603*, 1360.